Research Article

Parameter Analysis of Wall Thickness of Cured-in-Place Pipe Linings for Semistructured Rehabilitation of Concrete Drainage Pipe

Hongyuan Fang [1,2,3,4] **Kangjian Yang** [1,2,3] **Bin Li** [1,2,3] **Hang He** [1,2,3] **and Binghan Xue** [1,2,3]

[1]*School of Water Conservancy Engineering, Zhengzhou University, Zhengzhou 450001, China*
[2]*National Local Joint Engineering Laboratory of Major Infrastructure Testing and Rehabilitation Technology, Zhengzhou 450001, China*
[3]*Collaborative Innovation Center of Water Conservancy and Transportation Infrastructure Safety, Henan Province, Zhengzhou 450001, China*
[4]*Southern Engineering Inspection and Restoration Technology Research Institute, Huizhou 516029, China*

Correspondence should be addressed to Kangjian Yang; yangkangjian@gs.zzu.edu.cn and Binghan Xue; xuebinghan@zzu.edu.cn

Frequent accidents caused by underground pipeline damage are a widespread societal concern. Trenchless rehabilitation methods, particularly cured-in-place pipe (CIPP) lining, are increasingly used for pipeline repair with great success. Existing research is mainly concerned with practical improvements in rehabilitation and evaluating the performance of rehabilitation. In this study, the model of corroded buried concrete pipeline that had been rehabilitated with CIPP was established using numerical methods, and the Mesh-based parallel-Code Coupling Interface (MpCCI) was used to investigate multifield coupling effects of soil pressure, traffic load, and fluid-structure interactions. Moreover, the influences of corrosion depth, corrosion width, traffic load, cover depth, and water quantity on CIPP wall thickness were compared and analyzed. The result shows that maximum principal stress and vertical displacement of pipeline markedly decreased after CIPP rehabilitation, and thus the new CIPP can carry loads in a deteriorated pipe. Stress and displacement of the composite pipe liner were positively correlated with corrosion depth and negatively correlated with corrosion width. Increase in traffic load rapidly increases von Mises stress of CIPP, and increase in cover depth rapidly increases maximum principal stress of pipeline. Water flow has little effect on the pipe liner, and flow capacity increases slightly after CIPP rehabilitation. CIPP wall thickness was positively correlated with corrosion depth, traffic load, cover depth, and water quantity and negatively correlated with corrosion width.

1. Introduction

There are over 57.7 km of urban drainage pipelines in China, according to statistics published by the Ministry of Housing and Urban-Rural Development of PRC [1, 2]. Pipelines built before 2000 account for 44.97% of these. Failures from corrosion, rupture, and leakage are common due to years of neglect, and they cause frequent environmental accidents and road subsidence, which have considerable societal effects.

Open trench techniques, which can damage the environment and waste resources, are no longer feasible for buried pipeline maintenance and repair. Many trenchless pipeline rehabilitation methods, such as sliplining, pipe bursting, fold-and-form lining, deformed-and-reformed pipeline renewal, cured-in-place pipe (CIPP) lining, machine spiral wound lining, and splice segmental lining [3–7], have been developed in recent years to maintain and repair buried drainage pipes. CIPP technology is widely used

because it has the advantages of needing no grouting, rapid curing, and short construction time [8, 9]. The UV-CIPP process is to insert a resin-impregnated liner tube into a deteriorated buried pipeline and then to expand the liner and cure it in place, using ultraviolet light (UV), to produce a new pipe within a pipe. Figure 1 shows a schematic of UV-CIPP trenchless pipeline rehabilitation.

CIPP was first developed by a British engineer Eric Wood in 1971. The technology has achieved ISO 9000 international certification. There are many derived or related commercial technologies, such as Inliner and Superliner in the United States, Nordline in Belgium, MultiLing in Denmark, and AMEXR in Germany. A large amount of research has been devoted to improving the construction process and assuring the safety of CIPP technology. Matthews et al. [6, 10] described the use of CIPP to rehabilitate a 5,243 m length of 2,400 mm RC pipe and a 271 m length of 250 mm clay pipe in Texas. Many recommendations have been made to solve the problems encountered during installation. Allouche et al. [11] investigated the service life of a CIPP liner by examining the thickness of the annular gap, ovality, density, specific gravity, porosity, flexural strength, flexural modulus, tensile strength, tensile modulus, surface hardness, glass transition temperature, and Raman spectroscopy of liners that had been in use for 25, 23, 21, and 5 years. Alam et al. [12] created a database of performance data for rehabilitation technologies used in the water and wastewater sectors to assess CIPP service life. Straughan et al. [5] experimented on the long-term effects of external hydrostatic pressure on the structure of CIPP and FFP liners made by different manufacturers. Ra et al. [13] assessed the environmental impact of CIPP by investigating the volatile and semivolatile organic compound (VOC/SVOC) emissions from storm sewer CIPP installations. Zhong et al. [14] assessed the seismic performance and strength of straight buried pipelines in response to transient ground deformations using an experimentally validated hysteretic model of ductile iron push-on joints reinforced with CIPP liner. The research just described focuses on improving the construction and evaluating the performance of CIPP used for pipe rehabilitation.

Recent research has been concerned with the mechanics of pipe rehabilitation using CIPP [15]. Shou and Chen [16] investigated the effect of CIPP wall thickness on pipeline mechanics by analyzing the stress and displacement of buried corroded pipelines before and after CIPP repair, under various internal pressures and different surface loads, using Abaqus software. Chuk et al. [17] presented numerical analysis methods of stress for pipes lined with CIPP and analyzed the effects of different types of liner on pipe wall stress. Ji et al. [18] investigated the flexural modulus, strength, and deflection of a CIPP composite using a three-point bending apparatus. Argyrou et al. [19, 20] investigated the effect of abrupt ground movement caused by earthquake on CIPP by conducting a large-scale fault rupture test. They created a model based on the test results to analyze the axial elongation and bending of the pipeline, in which circumferential cracks and weak joints had been repaired by CIPP, under instantaneous ground deformation.

Currently, determining a reasonable wall thickness of CIPP liner that is both safe and economical has become a prominent research area. In this study, the Abaqus software, Fluent software, and MpCCI software were used to establish a model of corroded concrete pipeline repaired by CIPP that was subjected to the multifield coupling of soil pressure, traffic load, and fluid-structure interactions. The influences of corrosion depth, corrosion width, traffic load, cover depth, and water quantity on the composite pipe liner were analyzed. The results of this study provide a strong basis for designing of CIPP wall thickness.

2. 3D Finite Element Models

2.1. Structural Model. The structural model, which was created using Abaqus software, is a road structure containing a corroded buried concrete pipeline, UV-CIPP, and gaskets (Figure 2). The length, width, and depth of the model were 12 m, 8 m, and 8 m. The pavement layer of the road structure was 0.2 m deep, and the subgrade was 7.8 m deep. A linear elastic constitutive model was used for the pavement layer and UV-CIPP; the Mohr–Coulomb constitutive model was used for the subgrade; and the pipeline was described as a C30 typical concrete damaged plasticity model, as suggested by Lee and Fenves [21]. The gasket was a hyperelastic material modeled by the Mooney–Rivlin strain energy function. The material parameter values in Table 1 were selected according to reference [22]. Among them, C_{10}, C_{01}, and D_1 are Mooney constants related to temperature.

The elements of the structural model were meshed using Hypermesh 13.0 (Figure 3), with a minimum mesh size of 0.02 m and a maximum size of 0.1 m. Soil elements were densely meshed near the pipeline and sparsely meshed away from the pipeline. When the meshing was complete, the elements were exported from Hypermesh into Abaqus for calculation. Eight-node reduced-integration elements (C3D8R) and the enhanced hourglass control were used.

2.2. Pipeline Model. The un-remediated pipeline consisted of six pipe sections. The inside diameter of the pipe was 800 mm, the pipe wall thickness was 92 mm, the effective section length was 2,000 mm, and the detailed geometry of gasketed bell-and-spigot joints was selected according to the specification of the Chinese code for concrete and reinforced concrete sewer pipes [23], as shown in Figure 4(a). Oualita et al. [24] investigated the deterioration of 20-year-old buried concrete drainage pipes in Rennes. They determined the depassivation depth and the pH value at the crown, springline, and invert; the results showed that there was a significant loss of material at the crown while deterioration was the least at the invert. The main cause of depassivation was that the sulfate ions in the sewage are reduced by anaerobic bacterial action to hydrogen sulfide, which then dissolves in the water droplets generated at the crown, due to temperature differences, to produce sulfuric acid. The crown corrodes under the long-term action of sulfuric acid. Thus, the corrosion area in this study was located at the crown by
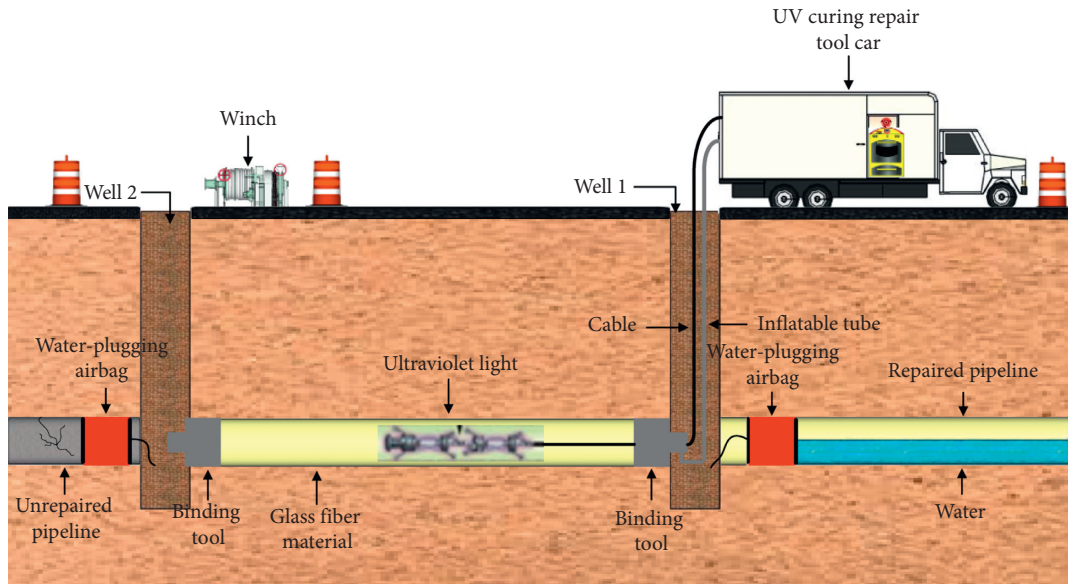
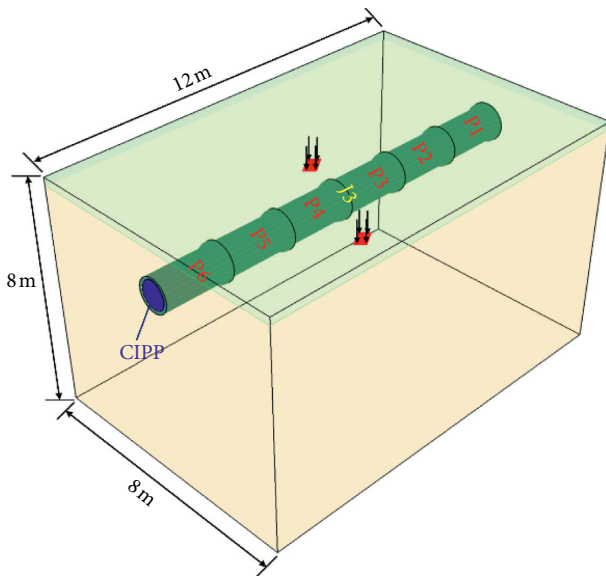Figure 1: UV-CIPP trenchless pipeline rehabilitation.

Figure 2: Three-dimensional finite element model.

Table 1: Material parameters and values.

Property	Value
Subgrade	
Density (kg/m^3)	1800
Elastic modulus (MPa)	50
Poisson's ratio	0.3
Cohesion (KPa)	18
Angle of internal friction (°)	30
Pavement layer	
Density (kg/m^3)	2400
Elastic modulus (MPa)	1200
Poisson's ratio	0.25
Concrete	
Density (kg/m^3)	2300
Elastic modulus (MPa)	30000
Poisson's ratio	0.2
Gasket	
Density (kg/m^3)	1200
C_{10} (Pa)	70000
C_{01} (Pa)	430000
D_1 (Pa^{-1})	$2.94E-5$

chiseling out the inner wall at the crown (Figure 4(b)), in which d_i is the corrosion depth, defined as the percentage of the original pipe wall, and α_i is the corrosion width, defined as the angle subtended at the pipeline in the vertical plane by the corrosion arc.

2.3. UV-CIPP Model. UV-CIPP consists of an outer coat, fiberglass fabric, and an inner membrane that is removed after curing. The outer coat adheres to the original pipeline after CIPP rehabilitation, thus forming a new composite concrete pipe-CIPP liner structure (referred to hereafter as the pipe liner), with an exterior of the original pipeline which resists the external load (Figure 5).

The UV-CIPP provides either semistructural or structural rehabilitation, according to the code of technical specifications for trenchless rehabilitation and renewal of urban sewer pipelines [25], depending on deterioration of the pipeline. Semistructural rehabilitation assumes that the original pipe can support the soil and surcharge loads throughout the design life of the rehabilitated pipe. Structural rehabilitation assumes that the original pipe is not structurally sound and cannot support soil or live loads or that it is likely to reach this condition over the design life of the rehabilitated pipe. In this study, the structural integrity of the pipeline was not compromised, and it could bear almost all external loads, so the wall thickness of the CIPP was determined with reference to the semistructural liner
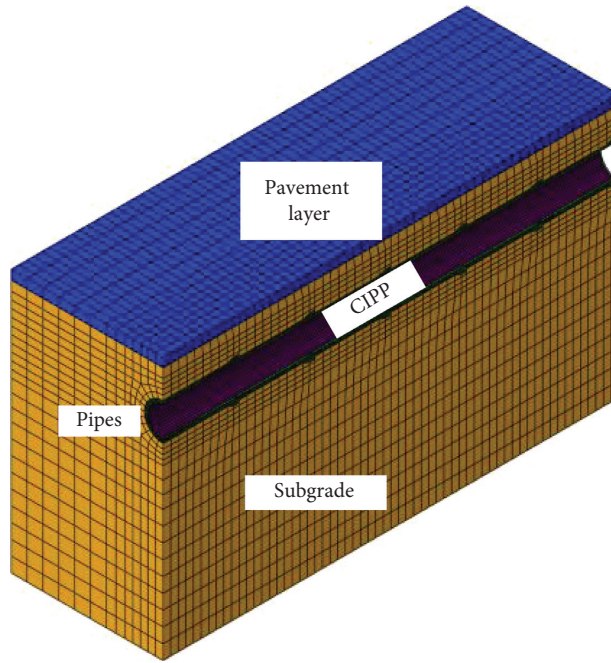
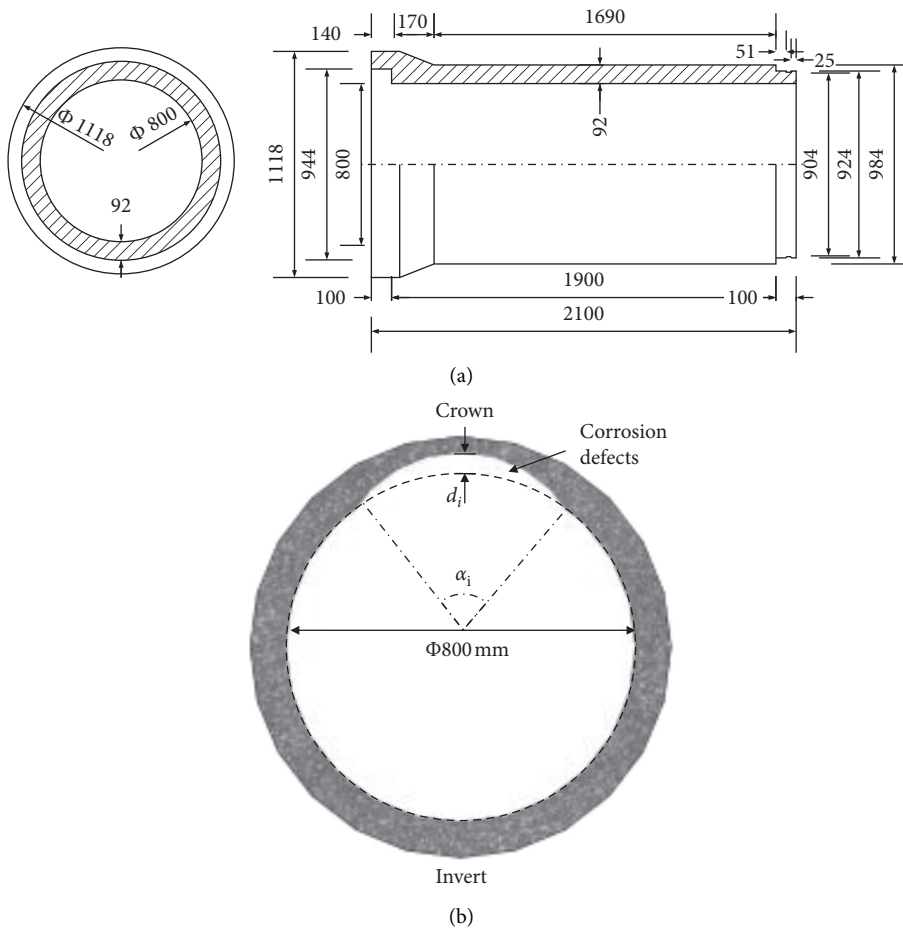FIGURE 3: Three-dimensional mesh geometry.

(a)

(b)

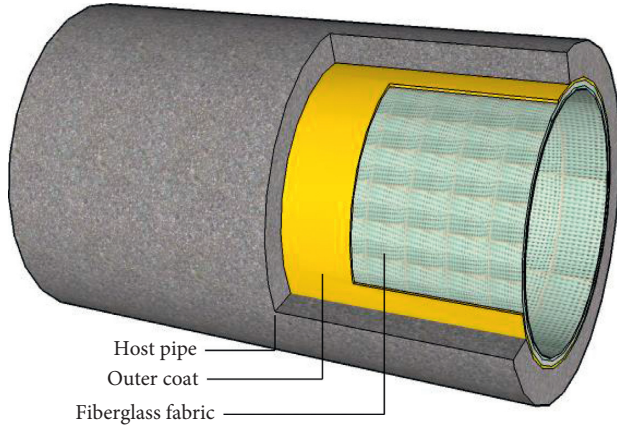FIGURE 4: (a) Pipe segment model and (b) corrosion depth and width.

Figure 5: Composite pipe liner structure formed by the original pipe and UV-CIPP.

Host pipe
Outer coat
Fiberglass fabric

design of the gravity pipe as shown in the following equation [26]:

$$t = \frac{D_0}{\left[2KE_L C/\left(PN\left(1 - \mu^2\right)\right)\right]^{(1/3)} + 1},$$ (1)

where t is the CIPP wall thickness (mm); D_0 is the inside diameter of the pipe, 800 mm; P is the groundwater load at the invert, 0.06 MPa; C is the ovality reduction factor, 0.84; N is the safety factor, 2.0; E_L is the long-term modulus of elasticity for CIPP, 8,800 MPa; K is the enhancement factor of the soil and existing pipe adjacent to the new pipe, 7.0; and μ is Poisson's ratio, 0.3.

The CIPP model with different thicknesses (based on equation (1)) was created to investigate the effects of CIPP wall thickness on the composite pipe liner structure. The outer diameter and total length (excluding the length of the bell of P1) of CIPP were 0.8 m and 11.9 m, respectively. The element size of CIPP is the same as the element size of the pipe, which is dense in the pipe crown and sparse in other locations. The CIPP model is shown in Figure 6. The mechanical properties of CIPP are shown in Table 2.

2.4. Traffic Load Model.
Wang [27] found that although traffic volume on a road varies over time, there is always some traffic on the road. Over time, vehicle load can be simplified as a uniform load with fixed magnitude and location. The Structural Design Code for Special Structures of Water Supply and Wastewater Engineering [28] stipulates that the traffic dynamic load can be simplified as a static load by multiplying it by a coefficient that is determined by the cover depth of the pipeline. Thus, we represented the traffic load, which acts on both sides of J3, as a uniform static load. The wheelbase and contact area of the traffic load were assumed to be 2.0 m and 0.21 m × 0.21 m.

2.5. Fluid Model.
Li et al. [29] found that the effect of fluid on the pipeline was limited but the coupled effects cannot be ignored. Thus, the fluid model was established to investigate the coupled effects on the mechanics of the composite structure using ANSYS software. Total length of the fluid was
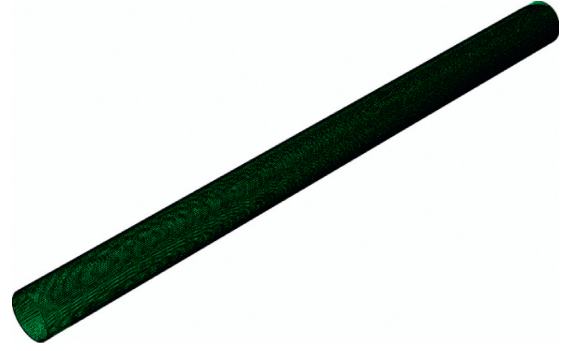

Figure 6: The CIPP model.

Table 2: The mechanical properties of CIPP.

Property	Value
Density (kg/m3)	1600
Elastic modulus (MPa)	8800
Poisson's ratio	0.3
Flexural strength (MPa)	31
Flexural modulus (MPa)	1724
Tensile strength (MPa)	21

11.9 m, and the outer diameter was the same as the inner diameter of the CIPP. Volume-of-fluid multiphase flow model was used to simulate gas-liquid flow in the pipeline, and RNG k–ε turbulence model was used to simulate fluid disorder, energy dissipation, and diffusion in the pipeline.

Water quantity was defined by equation (2), as specified in the Code for Design of Outdoor Wastewater Engineering [30]:

$$Q = \frac{H}{D},$$ (2)

where Q is water quantity, D is the pipeline diameter, and H is the height of water level.

After fluid geometry is established, the *ICEM CFD* method was used to divide the fluid into a hexahedral mesh with a minimum mesh size of 0.01 m and a maximum size of 0.05 m (Figure 7).

2.6. Model Interfaces.
There are four model interfaces: pipe-soil, pipe-gasket, pipe-liner, and liner-fluid. The normal behavior of the pipe-soil interaction was set to *Hard*, and tangential behavior was set to *Penalty*. The tangential friction coefficient μ was determined by the following equation:

$$\mu = \frac{A}{H/D - B} + C,$$ (3)

where H is the pipeline depth, D is the pipeline diameter, and A, B, and C are fitting parameters determined by the undrained shear strength of the soil. The values of A, B, and C were those used in [31], i.e., 0.756, 0.461, and 0.204, respectively.

Separation and slippage usually occur between pipe and gasket. The normal stiffness, shear stiffness, and friction
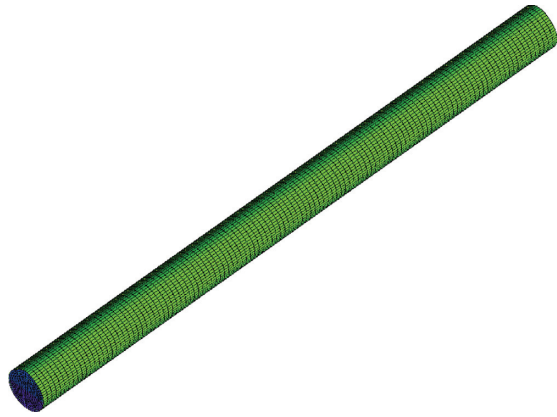
Figure 7: The fluid model.

angle for pipe-gasket interaction values were 10,000 GPa/m, 8,000 GPa/m, and 5°.

CIPP liner and host pipe can be well bonded, and there is a close fit between CIPP and the pipeline when CIPP is operating normally. Moreover, any deformation between pipe and CIPP can be remediated after CIPP rehabilitation. It is reasonable to assume that the displacement between CIPP and the original pipe is rather small and can be treated as zero. Thus, *Tie* was used to restrict displacement between the inside pipe wall and the outside CIPP wall.

Liner-fluid interaction was set in MpCCI using *overpressure*, which transfers the force and displacement at the liner-fluid interface, to simulate the behavior of CIPP and fluid.

2.7. Boundary Conditions

2.7.1. Boundary Conditions of the Structural Model. Displacement boundary conditions were set for soil, pipeline, and CIPP so that there was no movement on the bottom soil surface, no normal displacement on the surrounding soil surface, and no axial displacement on the pipe or CIPP.

2.7.2. Boundary Conditions of the Fluid Model. The water inlet, water outlet, air inlet, air outlet, and wall of the fluid were set using boundary conditions. The velocity inlet boundary was used as a water inlet, and velocity was set to 2 m/s. The outflow boundary was used as a water outlet, allowing fluid to flow freely. The pressure inlet and pressure outlet boundaries were used for air inlet and air outlet. The outlet pressure value was set to zero because the outlet was open to the atmosphere. The no slip boundary condition was used at the wall-fluid interface, and roughness was set to 0.01.

2.8. MpCCI Fluid-Solid Coupling. MpCCI is a software coupling environment which enables the exchange of data between the meshes of two different simulators. In this study, MpCCI was used to realize the coupling of the fluid model in Fluent and the structural model in Abaqus. The forces and displacements across the fluid-structure interfaces are used by MpCCI to perform coupled fluid-structure model calculations. The results can be analyzed with the postprocessing tools of each simulation code, with the FLUENT and ABAQUS visualizer (Figure 8).

2.9. Verification of the Numerical Model. Li et al. [29] carried out a full-scale test on the corroded concrete pipelines under multifield coupling effect. The corrosion depth was 30%, the corrosion width was 60°, the traffic load was 0.7 MPa, the cover depth was 1.0 m, and the water quantity was 0.5. The test plan is shown in Figure 9, and the material parameters of soil are shown in Table 3.

To obtain the circumferential strain of the exterior and interior walls of the pipe, the strain gauges were arranged in an eight-point star pattern on both the outside and inside of the walls of every section set on the pipe, as shown in Figure 10.

In order to verify the reliability of the numerical model in this study, a numerical model was established in this study based on Li's experiments. The circumferential strain of the section N1-N1 of the pipeline was extracted and analyzed, as shown in Figure 11. In the figure, FEA represents the finite element model data of pipeline, Test represents the data of Li's full-scale test.

It can be seen from Figure 11 that the numerical simulation results of circumferential strains are basically consistent with the results of Li's full-scale test in values and distribution trend, which indicates that the simulated parameter series (corroded depth = 30%, corroded depth = 60°, cover depth = 1 m, traffic load = 0.7 MPa, and water quantity = 0.5) was fully validated by Li's full-scale test. Therefore, it is reasonable to believe that the numerical model developed in this paper is reasonable and reliable.

3. Failure Criteria

The pipeline and CIPP are constructed from different materials and so have different failure characteristics. Different strength theory models were used to determine the failure characteristics.

The pipe is concrete, which has typical brittle characteristics; it will break under the action of external force when there is only a small deformation. According to the first strength theory, the fracture of concrete is determined by the following equation:

$$\sigma_1 = \sigma_u, \tag{4}$$

where σ_1 is the maximum principal stress of the component at the yield point and σ_u is the ultimate tensile strength of the concrete, which was selected as 1.4 MPa in this study.

Ji et al. [18] found that the CIPP liner has a large plastic yield before failure, which indicates that the material of CIPP has significant plastic characteristics. According to the fourth strength theory, plastic yield of the CIPP is determined by the following equation:

$$\sqrt{\frac{1}{2}\left[(\sigma_1 - \sigma_2)^2 + (\sigma_2 - \sigma_3)^2 + (\sigma_1 - \sigma_2)^2\right]} = \sigma_s, \tag{5}$$
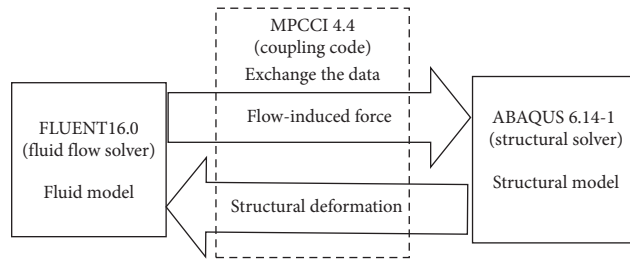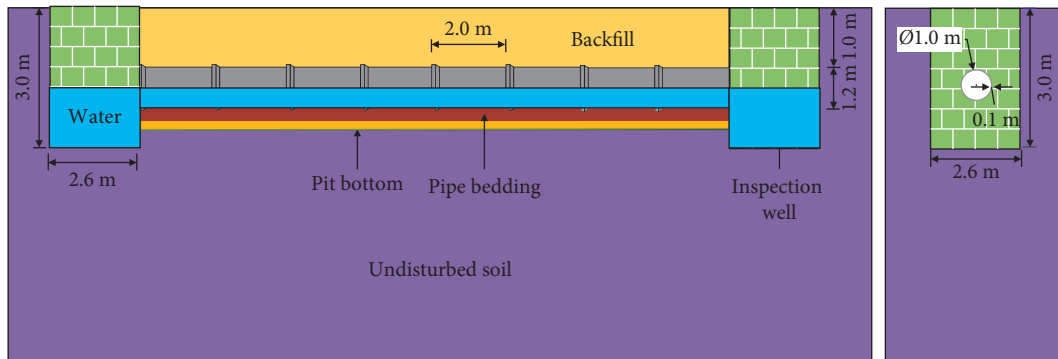
Figure 8: The MpCCI solution.

Figure 9: Test plan.

Table 3: Properties of backfill material tested.

Property	Value
Maximum dry density (kg/m^3)	1732
Modulus of elasticity (MPa)	43.50
Peak angle of internal friction (°)	25.20
Natural water content	20.71
Liquid limit (%)	22.90
Plastic limit (%)	14.70

where σ_1, σ_2, and σ_3 are the three principal stresses at the yield point and σ_s is the yield limit of the material, which was selected as 21 MPa in this study.

4. Numerical Results and Discussion

4.1. Effect of Corrosion Depth. This section discusses the effect of corrosion depth on the composite pipe liner. Corrosion width was 60°, cover depth was 1 m, traffic load was 0.75 MPa, and water quantity was 0.5. Different corrosion depths were simulated in the pipe by chiseling out the inside of the pipe wall to different depths. Pipelines with corrosion depths of 10%, 30%, and 50% were each repaired by CIPP with wall thicknesses of 0 mm, 3 mm, 6 mm, 9 mm, 12 mm, and 15 mm. The maximum values of maximum principal stress and vertical pipe displacement and the maximum values of von Mises stress and vertical CIPP displacement were compared and analyzed (Figures 12 and 13).

Figure 12 shows that maximum principal stress and vertical displacement of pipeline were positively correlated with corrosion depth and negatively correlated with CIPP wall thickness. When CIPP wall thickness increased from

0 mm to 3 mm, both maximum principal stress and vertical displacement greatly decreased. It can be concluded that the marked decrease in maximum principal stress and vertical displacement indicates that the pipeline becomes much safer after CIPP rehabilitation. As CIPP wall thickness increased, maximum principal stress and vertical displacement decreased gradually, which indicates that increased CIPP wall thickness increases the structural integrity of the composite pipe liner.

Figure 13 shows that as corrosion depth increased, both von Mises stress and vertical displacement of CIPP gradually increased. As CIPP wall thickness increased, the von Mises stress and vertical displacement initially decreased rapidly (3 mm–6 mm), then decreased slowly (6 mm–9 mm), and finally decreased gently (9 mm–15 mm). We explain this as follows: the force analysis of CIPP can be approximated by a model of a long cylinder subjected to uniform circumferential pressure outward, with a critical pressure $P_{cr} = 2.2(t/D_0)3$. P_{cr} indicates that when wall thickness t is small, CIPP is rather unstable, so CIPP stress is large. When wall thickness reaches a certain value, the structure becomes stable, and further increase in wall thickness has little effect on CIPP stress in the case of constant external load. This analysis shows that there is a reasonable range of CIPP wall thickness that can meet the requirements of both safety and economy.

A comparison of Figure 12(a) with Figure 13(a) shows that vertical displacement between pipe and CIPP is almost constant and the difference in vertical displacement between them does not exceed 0.01 mm, which indicates that the pipeline and CIPP behave synchronously. A comparison of Figure 12(b) with Figure 13(b) shows that the effect of corrosion depth is more significant than that of CIPP.
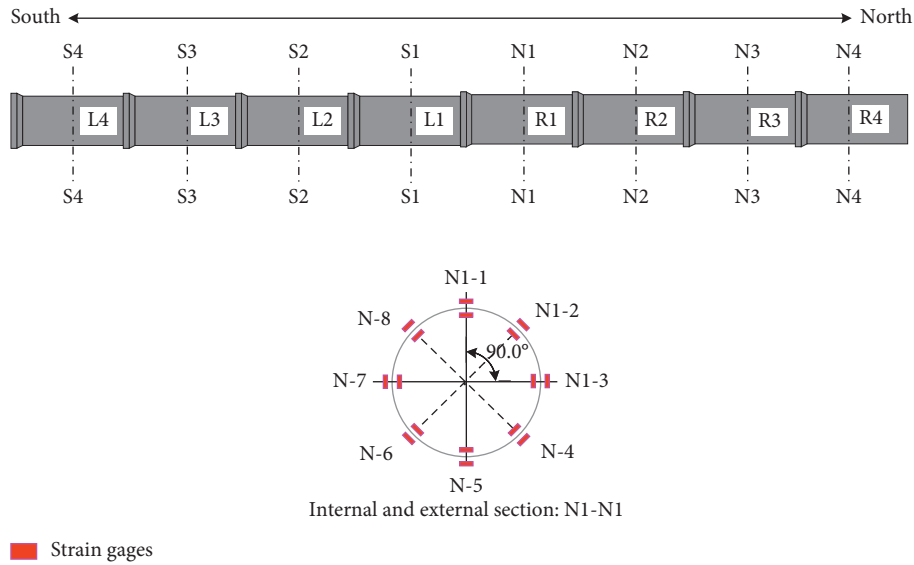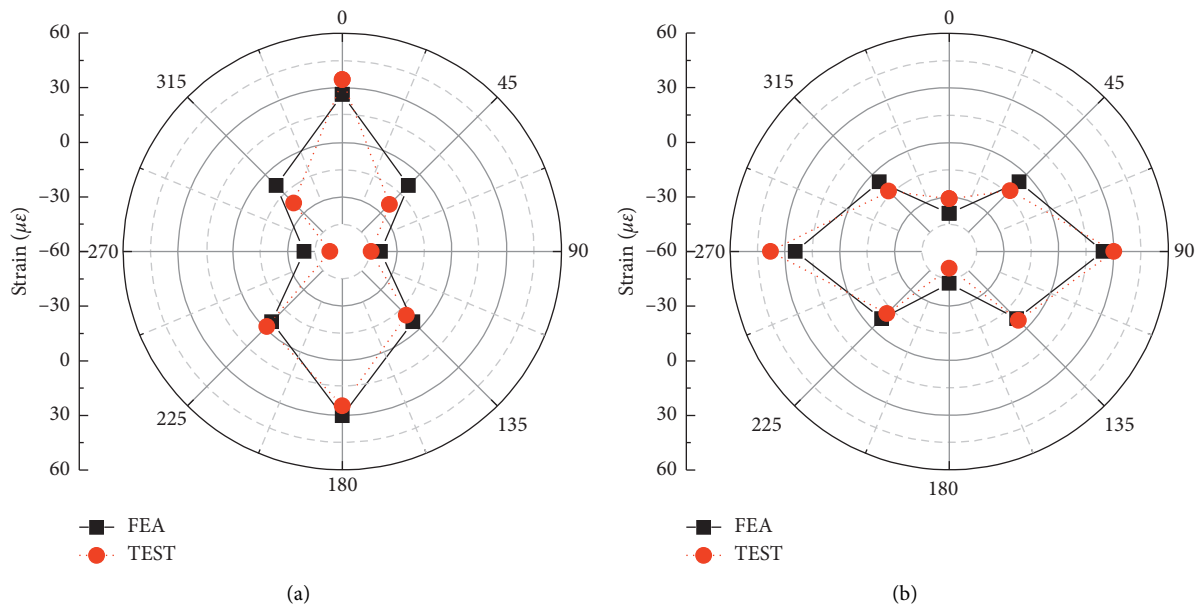
Figure 10: Strain gauge configuration.

Figure 11: Circumferential strain of corroded pipeline under multifield coupling: (a) interior and (b) exterior.

Although corrosion depth increases, the pipeline, which is not structurally damaged and maintains rigidity, can still bear external loads, such as soil pressure and traffic loads, and provide structural support for CIPP. Therefore, increased corrosion depth has a greater effect on the pipeline than it has on CIPP.

4.2. Effect of Corrosion Width. Corrosion depth, cover depth, traffic load, and water quantity were set to 30%, 1 m, 0.75 MPa, and 0.5. Different corrosion widths were set by changing the arc length that subtends the angle of corrosion

at the pipeline. Pipelines with corrosion widths 30°, 60°, and 90° were each repaired by CIPP with wall thicknesses 0 mm, 3 mm, 6 mm, 9 mm, 12 mm, and 15 mm. Maximum values of stress and vertical displacements of pipeline and CIPP were compared and analyzed (Figures 14 and 15).

Figure 14 shows that maximum principal stress and vertical displacement of pipeline were negatively correlated with corrosion width and that the influence of corrosion width on maximum principal stress was significantly greater than that on vertical displacement. Concrete pipe rigidity was unchanged as corrosion width increased, so corroded pipes have only slight deformation under external loads. The
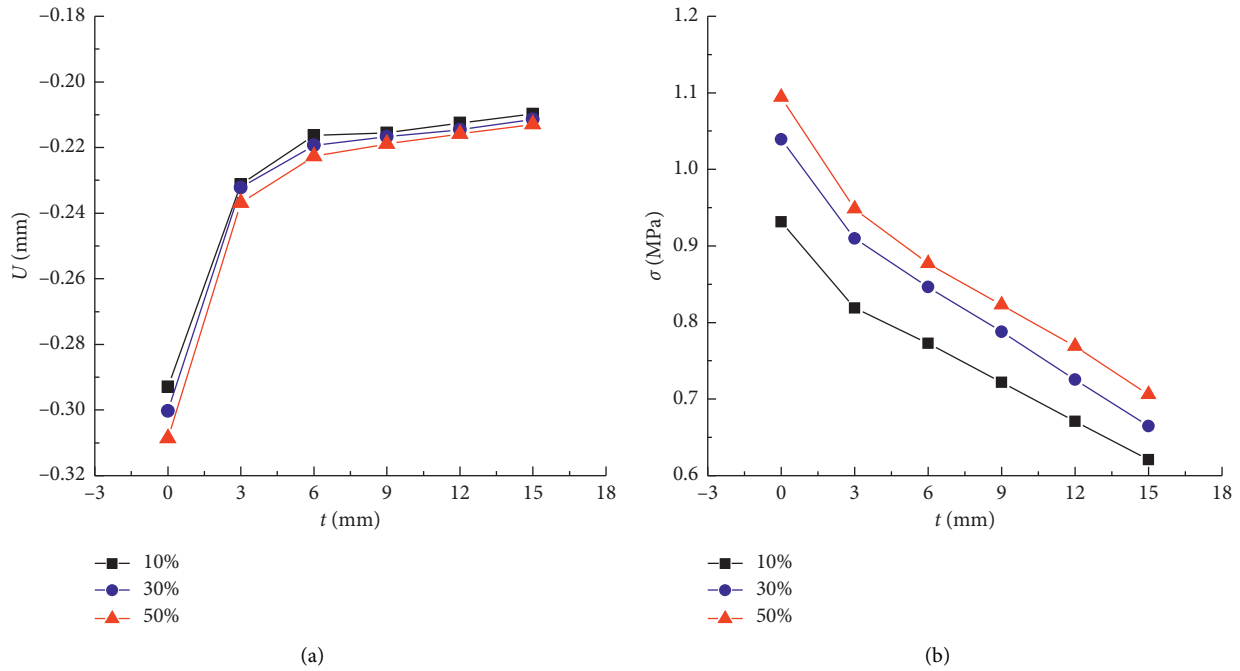
(a)

(b)

FIGURE 12: The relationship between CIPP wall thickness and (a) vertical displacement and CIPP wall thickness and (b) maximum principal stress of pipeline for different corrosion depths.
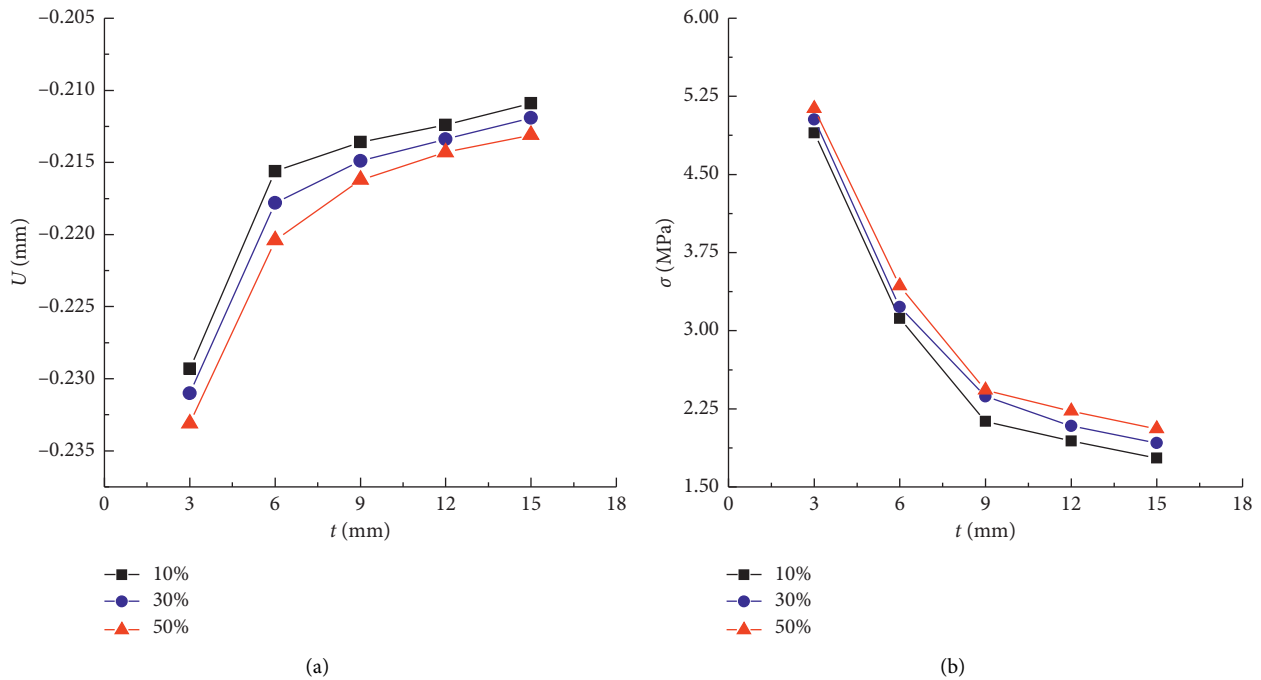

(a)

(b)

FIGURE 13: The relationship between CIPP wall thickness and (a) vertical displacement and CIPP wall thickness and (b) von Mises stress of CIPP for different corrosion depths.

change in corrosion width had no significant effect on vertical displacement.

Figure 15 shows that von Mises stress and vertical displacement of CIPP were negatively correlated with corrosion width. The main reason is as follows: when corrosion width was small, stress was concentrated in the pipe liner, which led

to a rapid increase in stress of the composite structure. As corrosion width increased, stress concentration was reduced, so stress and vertical displacement of the pipe liner decreased accordingly. It can be concluded that stress and vertical displacement of the pipe liner were negatively correlated with corrosion width. The probability of failure in the pipe liner is
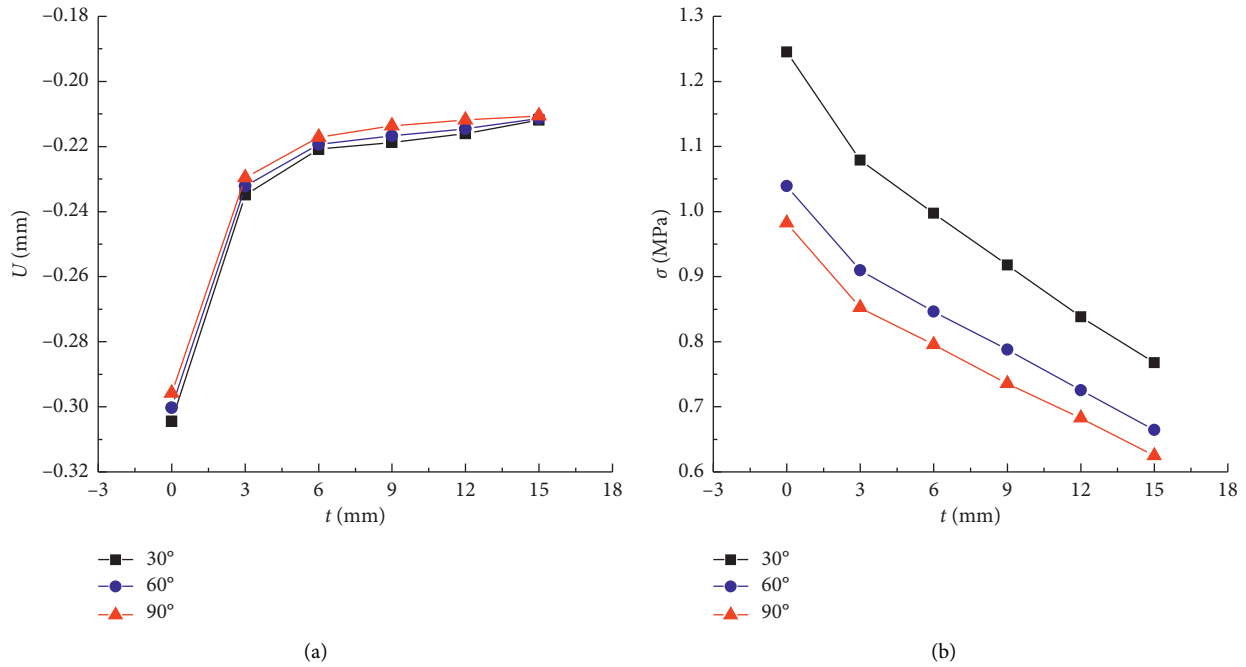
(a)

(b)

Figure 14: The relationship between CIPP wall thickness and (a) vertical displacement and CIPP wall thickness and (b) maximum principal stress of pipeline for different corrosion widths.
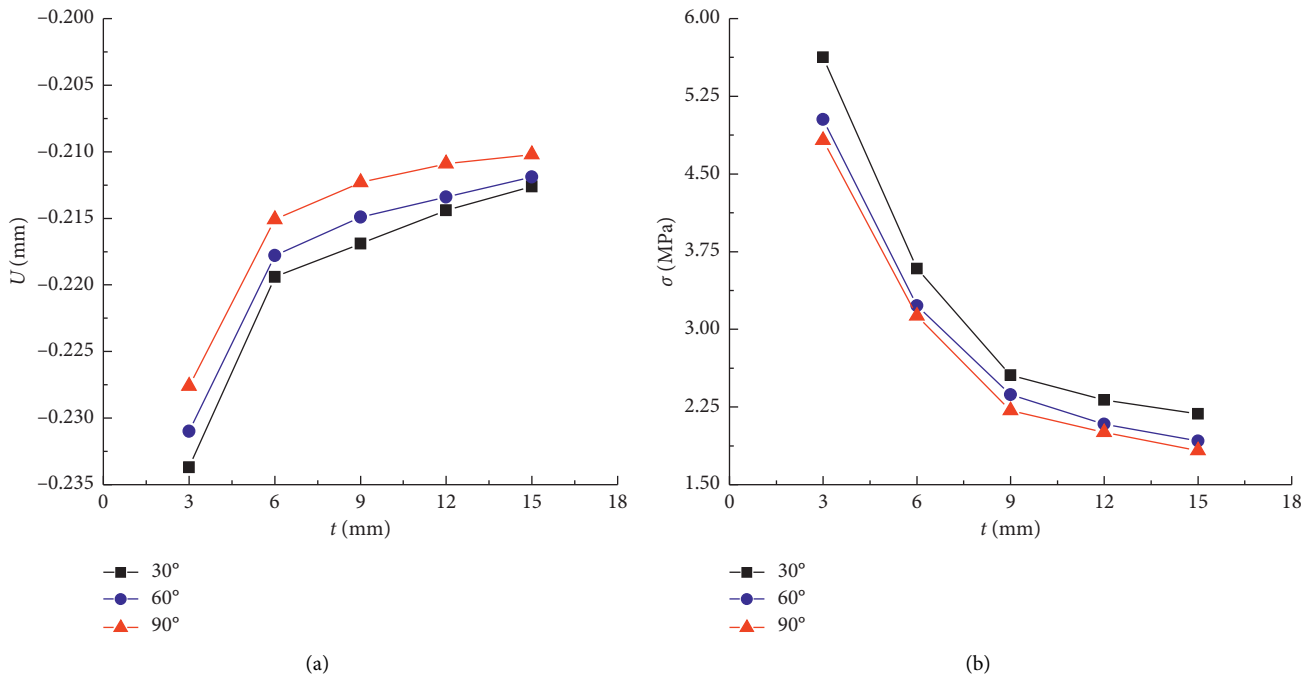

(a)

(b)

Figure 15: The relationship between CIPP wall thickness and (a) vertical displacement and CIPP wall thickness and (b) von Mises stress of CIPP for different corrosion widths.

greater when corrosion width is smaller. Thus, the CIPP wall should be thicker when corrosion width is smaller.

4.3. Effect of Traffic Load. To investigate the effect of different traffic loads on the mechanical properties of the pipe liner, pipelines that were repaired using CIPP with wall thicknesses of 0 mm, 3 mm, 6 mm, 9 mm, 12 mm, and 15 mm using the traffic loads of 0.5 MPa, 0.75 MPa, and 1.0 MPa were modeled. Corrosion depth and corrosion width were 30% and 60°. Cover depth was 1 m, and water quantity was 0.5. Maximum value of stress and vertical displacement of pipeline and CIPP were compared and analyzed (Figures 16 and 17).
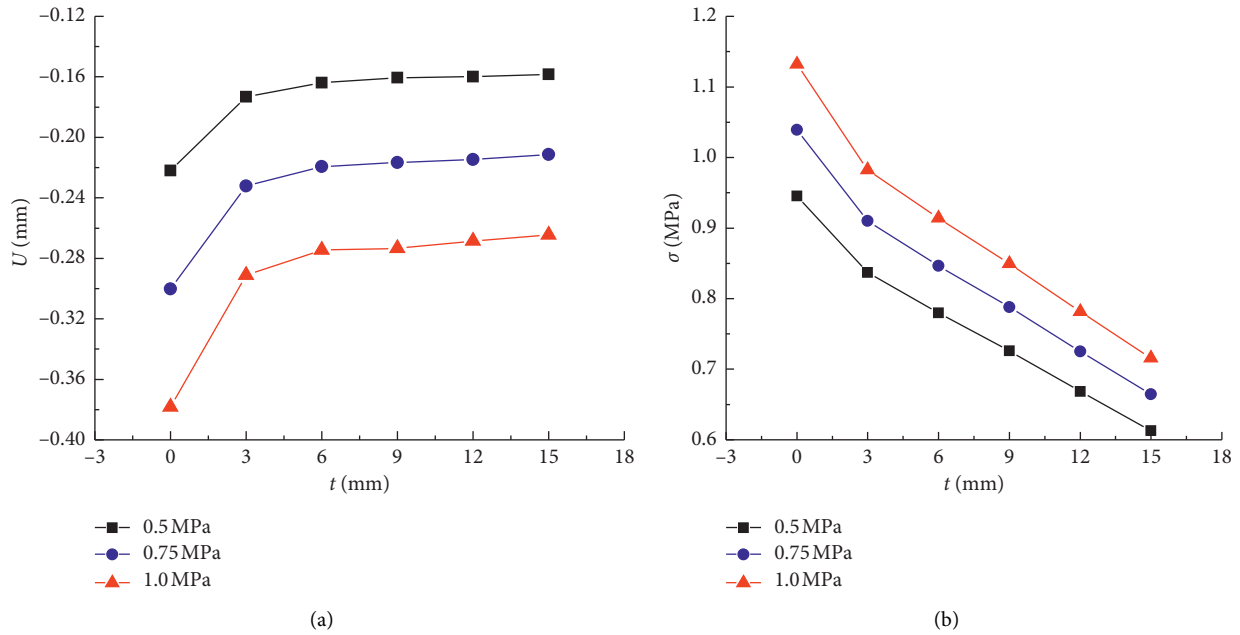
FIGURE 16: The relationship between CIPP wall thickness and (a) vertical displacement and CIPP wall thickness and (b) maximum principal stress of pipeline for different traffic loads.
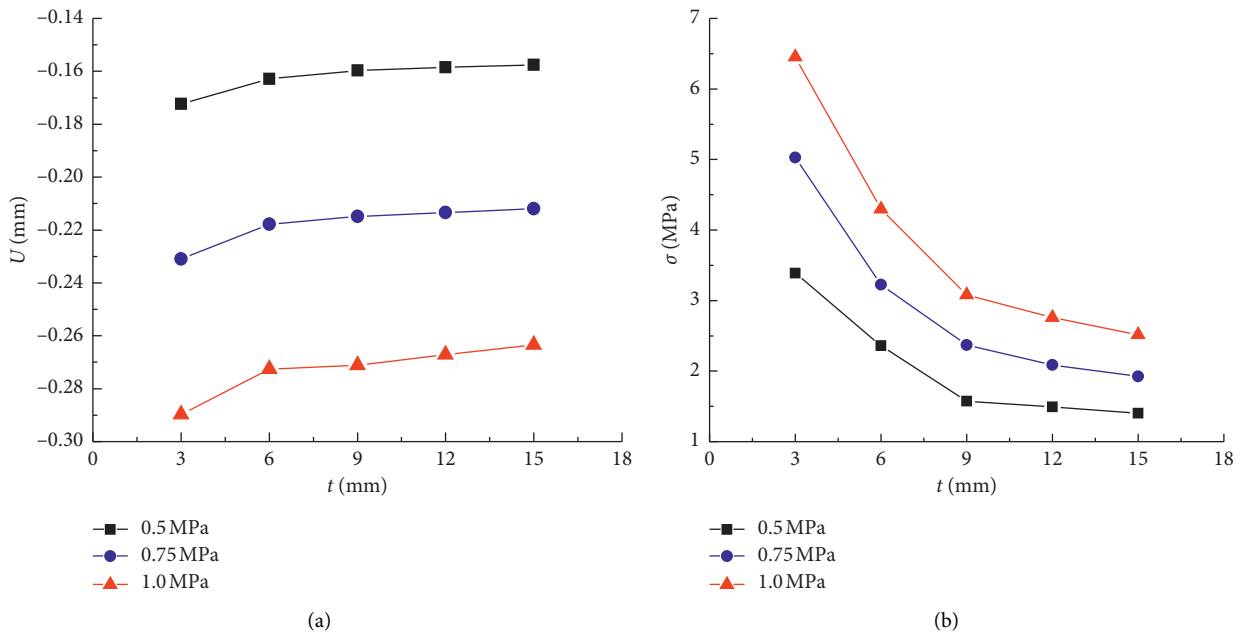

FIGURE 17: The relationship between CIPP wall thickness and (a) vertical displacement and CIPP wall thickness and (b) von Mises stress of CIPP for different traffic loads.

Figures 16 and 17 show that stress and vertical displacement of pipeline and CIPP increased as traffic load increased. When CIPP wall thickness was 9 mm, traffic load increased from 0.5 MPa to 0.75 MPa, maximum principal stress and vertical displacement of pipeline increased by factors of 1.085 and 1.349, and von Mises stress and vertical displacement of CIPP increased by factors of 1.507 and 1.346. When traffic load increased from 0.75 MPa to 1.0 MPa, maximum principal stress and vertical displacement of pipeline increased by factors of 1.078 and 1.262 and von Mises stress and vertical displacement of CIPP increased by factors of 1.301 and 1.262. Traffic load had a great effect on the pipe liner, but the effect of traffic load on CIPP was more significant than the effect of the pipeline. The main reason is as follows: traffic load has a significant effect on joint rotation but joint rotation will be reduced after CIPP installation.
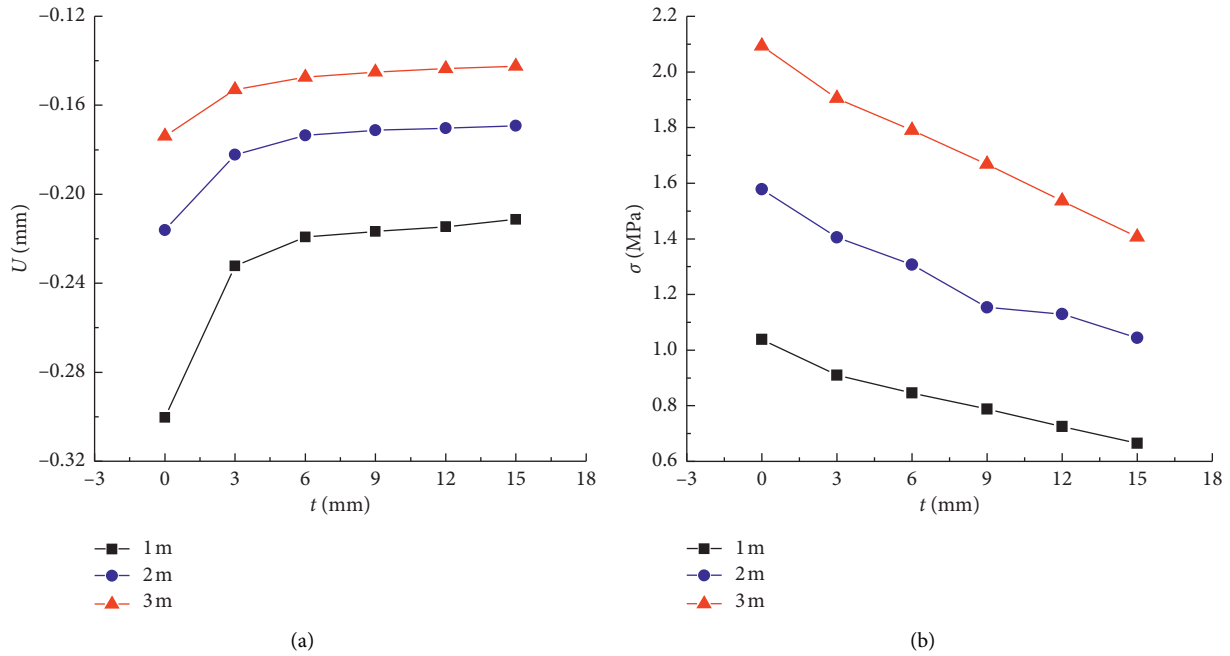
FIGURE 18: The relationship between CIPP wall thickness and (a) vertical displacement and CIPP wall thickness and (b) maximum principal stress of pipeline for different cover depths.
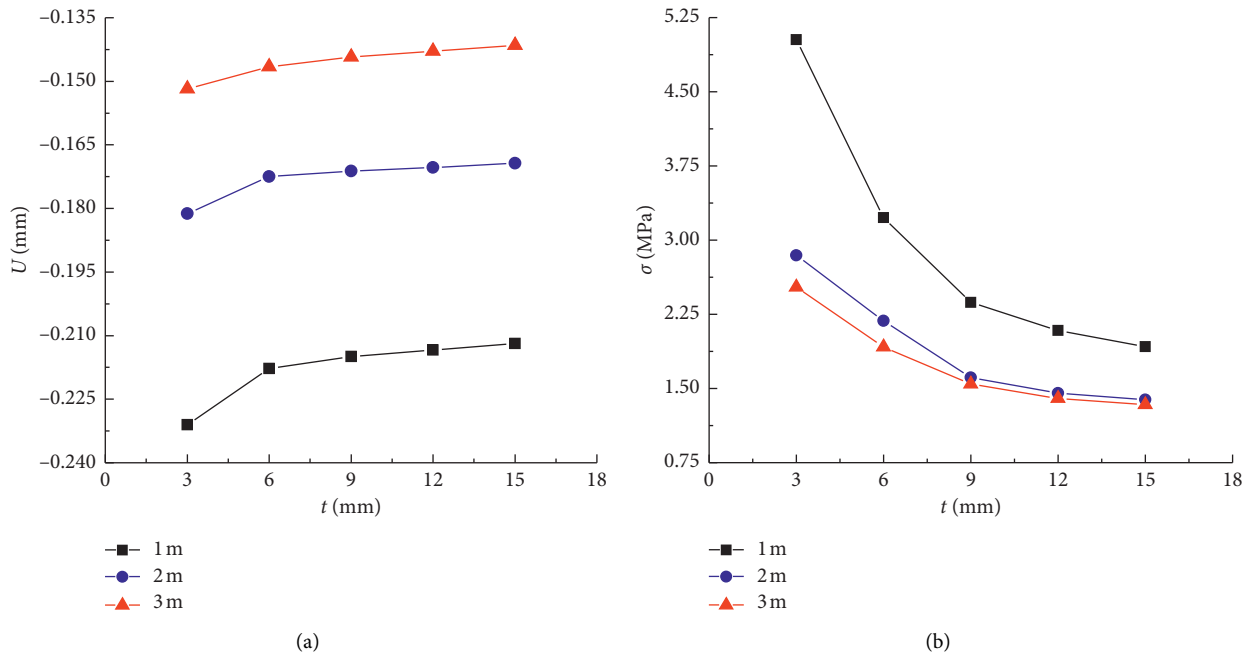

FIGURE 19: The relationship between CIPP wall thickness and (a) vertical displacement and CIPP wall thickness and (b) von Mises stress of CIPP for different cover depths.

This results in stress concentration on CIPP at the pipe joints, and thus an increase in traffic load will cause a rapid increase in CIPP stress. Traffic load has a great influence on the composite pipe liner. Greater traffic load increases the risk of damage to the pipe liner, so the thickness of the CIPP should be increased to compensate.

4.4. Effect of Cover Depth. The pressure from the covering infill is an important permanent load on a pipeline and greatly influences pipeline design. Pipelines repaired by CIPP with wall thicknesses of 0 mm, 3 mm, 6 mm, 9 mm, 12 mm, and 15 mm using cover depths of 1m, 2 m, and 3 m were modeled. Corrosion depth and corrosion width were
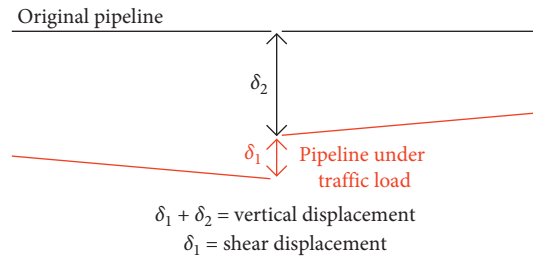
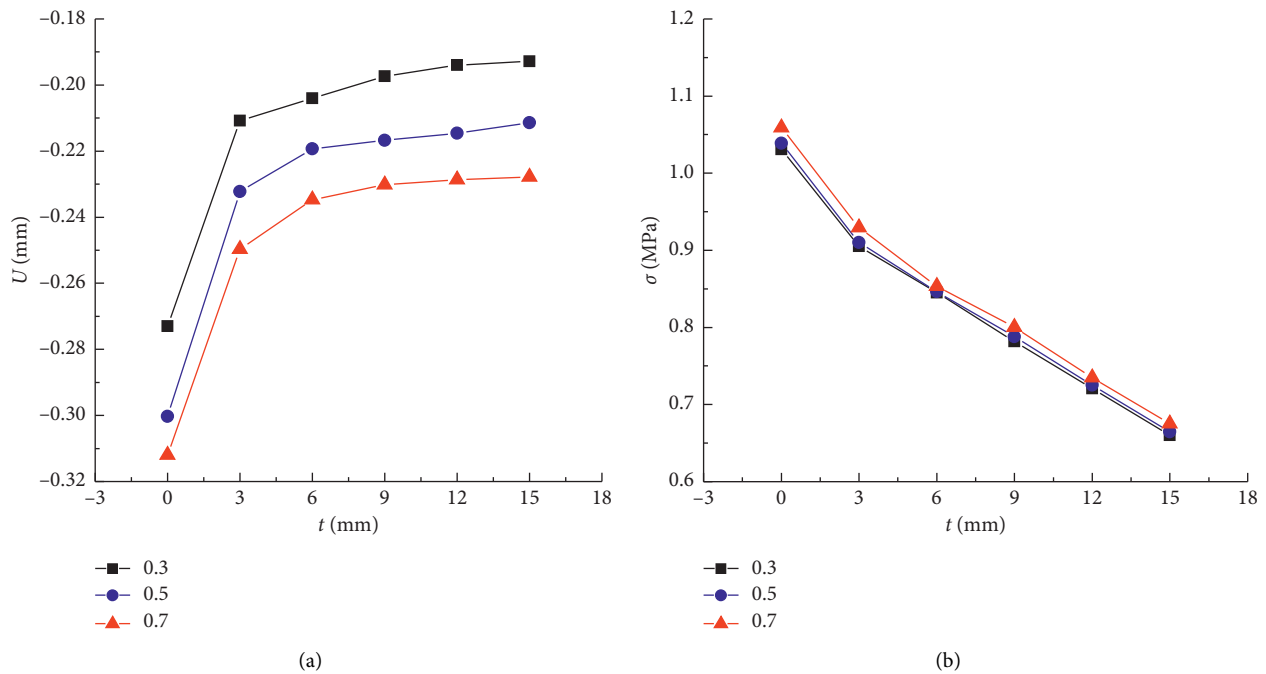FIGURE 20: The diagram of vertical displacement and shear displacement.

FIGURE 21: The relationship between CIPP wall thickness and (a) vertical displacement and CIPP wall thickness and (b) maximum principal stress of pipeline for different water quantities.

30% and 60°. Traffic load was 0.75 MPa, and water quantity was 0.5. Maximum value of stress and vertical displacements of pipeline and CIPP were compared and analyzed (Figures 18 and 19).

Figures 18(a) and 19(a) show that vertical displacement of pipeline and CIPP decreased as cover depth increased. The original pipeline had been buried for many years, and the surrounding soil was already consolidated and stable before CIPP rehabilitation. The vertical displacement of the pipe liner is therefore mainly caused by traffic loads, and the cover depth has little effect on it. The infill dissipates the traffic load, so the vertical displacement of the pipe liner decreased as the cover depth increased.

Figures 18(b) and 19(b) show that maximum principal stress of pipeline increased as cover depth increased, but von Mises stress of CIPP decreased as cover depth increased. The main reason is as follows: pressure on the pipe increased as the cover depth increased, which is seen as an increase in

maximum principal stress. However, the pipe is still able to withstand almost all the pressure and thus provides structural support for CIPP, so the covering pressure has little effect on the CIPP. Xu et al. [32] observed that the longitudinal deformation of a jointed pipeline was highly discontinuous, due to the asymmetric geometry of the bell and spigot at the joint, and that rotation and shear displacement were concentrated at the joints. The diagram of vertical displacement and shear displacement is shown in Figure 20.

Figure 20 shows that the difference in vertical displacement caused by the asymmetric geometry of the bell and spigot will lead to shear displacement of the CIPP, resulting in a rapid increase in the stress of the CIPP. An increase of vertical displacement will cause the difference of vertical displacement to increase. So, CIPP stress was negatively correlated with vertical displacement: CIPP stress decreased as cover depth increased. The failure of the pipe liner should take into account the cracking of the pipe and
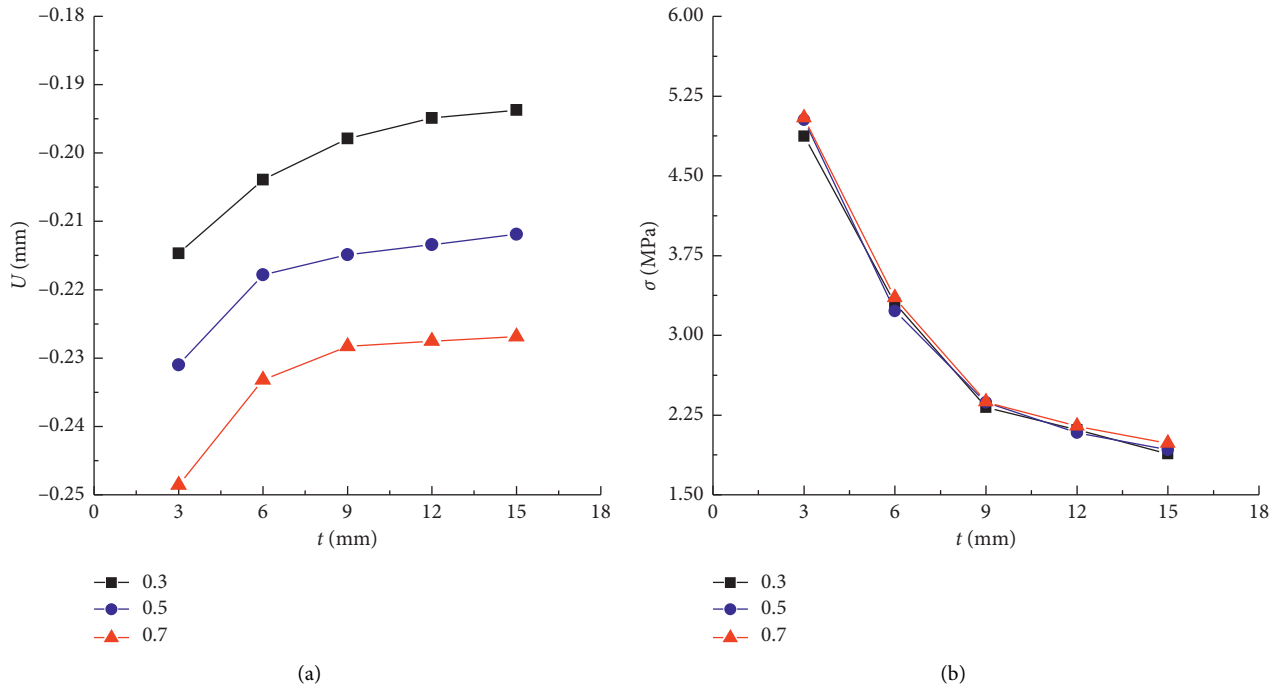
(a)

(b)

FIGURE 22: The relationship between CIPP wall thickness and (a) vertical displacement and CIPP wall thickness and (b) von Mises stress of CIPP for different water quantities.

the yield of the CIPP. Although an increase in the cover depth can reduce the von Mises stress of CIPP, it will rapidly increase the maximum principal stress of pipeline. This increase will result in the maximum principal stress of pipeline quickly reaching the ultimate tensile strength of the concrete and thus increase the risk of the pipe cracking. Therefore, the thickness of CIPP should be increased for greater cover depths to ensure that the maximum principal stress of the pipeline is in a safe range.

4.5. Effect of Water Quantity. The effect of water quantity on CIPP wall thickness is described in this section. Pipelines that were rehabilitated by CIPP with wall thicknesses of 0 mm, 3 mm, 6 mm, 9 mm, 12 mm, and 15 mm with water quantities of 0.3, 0.5, and 0.7 were modeled. Corrosion depth and corrosion width were 30% and 60°. Traffic load was 0.75 MPa, and cover depth was 1.0 m. Maximum value of stress and vertical displacements of pipeline and CIPP were compared and analyzed (Figures 21 and 22).

Figures 21 and 22 show that stress and vertical displacement of pipeline and CIPP increased as water quantity increased. At CIPP wall thickness of 9 mm, when water quantity increased from 0.3 to 0.5, maximum principal stress and vertical displacement of pipeline increased by factors of 1.008 and 1.098 and von Mises stress and vertical displacement of CIPP increased by factors of 1.008 and 1.085. When water quantity increased from 0.5 to 0.7, maximum principal stress and vertical displacement of pipeline increased by factors of 1.014 and 1.062 and von Mises stress and vertical displacement of CIPP increased by factors of 1.003 and 1.062. It can be concluded that water quantity has

little effect on the pipe liner. An [33] calculated the increased flow capacity of a pipeline after CIPP rehabilitation and found that it increased by 14.3% over that of the original pipeline. The main reason is as follows: the increase occurs because the roughness coefficient of CIPP is less than that of the original pipeline and the CIPP wall is not very thick, so there is less resistance to flow and little reduction in pipe cross-sectional area. So, the effect of water quantity on the thickness of the CIPP wall was investigated only through a mechanical analysis of the pipe liner, and it can be concluded that CIPP wall thickness should be increased as water quantity increases.

5. Conclusion

In this study, the three-dimensional numerical model of a corroded buried concrete drainage pipeline that had been rehabilitated with CIPP was established and the effects of various factors on the thickness of the CIPP wall were analyzed. The principal findings of our research are summarized as follows:

(1) Maximum principal stress and vertical displacement of pipeline decreased notably after CIPP rehabilitation, so rehabilitated pipeline is much safer than the original, and CIPP wall thickness was positively correlated with corrosion depth, traffic load, cover depth, and water quantity and negatively correlated with corrosion width.

(2) Stress and displacement of the composite pipe liner were positively correlated with corrosion depth and negatively correlated with corrosion width. The

effects of corrosion depth and corrosion width on the pipeline are significantly greater than the effects of CIPP.

(3) The parameters of traffic load and cover depth should be taken into account when planning to rehabilitate concrete drainage pipes. Traffic load and cover depth greatly affect the composite pipe liner structure. Increase in traffic load rapidly increases von Mises stress of CIPP, and increase in cover depth rapidly increases maximum principal stress of pipeline.

(4) Shear displacement, which rapidly increases CIPP stress, is mainly caused by traffic load and is little affected by cover depth. Cover depth dissipates traffic load, so von Mises stress of CIPP decreases as cover depth increases.

(5) Water flow has little effect on the pipe liner, and flow capacity increases slightly after CIPP rehabilitation. From our analysis of the mechanical effects of water quantity on the pipe liner, it is recommended that CIPP wall thickness should be increased as water quantity increases.

6. Recommendations for Future Research

CIPP technology has great advantages in nonexcavation repair of pipelines because it has the advantages of short construction time and good repair effect and it does not reduce the flow capacity of pipeline. However, the mechanical response and long-term service performance of CIPP composite pipe liner structure under multifield coupling have not been fully revealed. Therefore, we have some suggestions for the future research on CIPP.

(1) There is a range of CIPP wall thicknesses that are both safe and economical, which needs to study not only the influence of various factors on the composite pipe liner structure but also the relationship between the repair cost and wall thickness of CIPP.

(2) The field pipe samples repaired by CIPP should be tested in the laboratory to evaluate the effect of CIPP rehabilitation.

(3) The effects of wall thickness of CIPP on other common types of pipe materials such as HDPE, PVC, and DIP should also be examined.

Data Availability

The data used to support the findings of this study are included within the article. In addition, the finite element models are available from the corresponding author upon request.

Conflicts of Interest

The authors declare that there are no conflicts of interest regarding the publication of this paper.

References

[1] G. F. An, *Technical Guide for Trenchless Rehabilitation Engineering of Urban Sewer Pipeline*, China Architecture & Building Press, Beijing, China, 2015.

[2] B. S. Ma, *Trenchless Pipeline Rehabilitation and Renewal Technology*, China Communications Press, Beijing, China, 2014.

[3] D. I. Garcia, "Sliplining rehabilitation approaches for large force mains," *Proceedings of the Water Environment Federation*, vol. 2017, no. 2, pp. 253–269, 2017.

[4] S. Adamtey and L. Onsarigo, "Analysis of pipe-bursting construction risks using probability-impact model," *Journal of Engineering, Design and Technology*, vol. 16, no. 3, pp. 461–477, 2018.

[5] W. T. Straughan, L. K. Guice, and C. Mal-Duraipandian, "Long-term structural behavior of pipeline rehabilitation systems," *Journal of Infrastructure Systems*, vol. 1, no. 4, pp. 214–220, 1995.

[6] J. C. Matthews, "Large-diameter sewer rehabilitation using a fiber-reinforced cured-in-place pipe," *Practice Periodical on Structural Design and Construction*, vol. 20, no. 2, Article ID 04014031, 2014.

[7] R. Ishmuratov, O. Vladimir, and A. Alexey, "The spiral wound pipeline rehabilitation technique for pipe networks: an application and experience in Moscow city," *International No-Dig*, vol. 31, pp. 1–7, 2013.

[8] Z. Zhong, A. Filiatrault, and A. Aref, "Experimental performance evaluation of pipelines rehabilitated with cured-in-place pipe liner under earthquake transient ground deformations," *Journal of Infrastructure Systems—ASCE*, vol. 23, no. 2, 2017.

[9] Z. Zhong, S. Wang, M. Zhao, X. Du, and L. Li, "Performance of ductile iron push-on joints rehabilitated with CIPP liner under repetitive and seismic loadings," *Soil Dynamics and Earthquake Engineering*, vol. 115, pp. 776–786, 2018.

[10] J. Matthews, "Sewer rehabilitation using an ultraviolet-cured GFR cured-in-place pipe," *Practice Periodical on Structural Design and Construction*, vol. 20, no. 1, Article ID 04014021, 2013.

[11] E. Allouche, S. Alam, J. Simicevic et al., "A pilot study for retrospective evaluation of cured-in-place pipe (CIPP) rehabilitation of municipal gravity sewers," *Tunnelling and Underground Space Technology*, vol. 39, pp. 82–93, 2014.

[12] S. Alam, R. L. Sterling, E. Allouche et al., "A retrospective evaluation of the performance of liner systems used to rehabilitate municipal gravity sewers," *Tunnelling and Underground Space Technology*, vol. 50, pp. 451–464, 2015.

[13] K. Ra, S. M. Teimouri Sendesi, M. Nuruddin et al., "Considerations for emission monitoring and liner analysis of

thermally manufactured sewer cured-in-place-pipes (CIPP)," *Journal of Hazardous Materials*, vol. 371, pp. 540–549, 2019.

[14] Z. Zhong, A. Filiatrault, and A. Aref, "Numerical simulation and seismic performance evaluation of buried pipelines rehabilitated with cured-in-place-pipe liner under seismic wave propagation," *Earthquake Engineering & Structural Dynamics*, vol. 46, no. 5, pp. 811–829, 2017.

[15] S.-S. Jeon, T. D. O'Rourke, and A. N. Neravali, "Repetitive loading effects on cast iron pipelines with cast-in-place pipe lining systems," *Journal of Transportation Engineering*, vol. 130, no. 6, pp. 692–705, 2004.

[16] K. J. Shou and B. C. Chen, "Numerical analysis of the mechanical behaviors of pressurized underground pipelines rehabilitated by cured-in-place-pipe method," *Tunnelling and Underground Space Technology*, vol. 71, pp. 544–554, 2018.

[17] C. Chuk, G. Urgessa, and H. Thippeswamy, "Numerical analysis of stresses for cured-in-place-pipe linings," *WIT Transactions on The Built Environment*, vol. 71, pp. 283–293, 2011.

[18] H. Ji, S. Yoo, J. Kim, and D. Koo, "The mechanical properties of high strength reinforced cured-in-place pipe (CIPP) liner composites for urban water infrastructure rehabilitation," *Water*, vol. 10, no. 8, p. 983, 2018.

[19] C. Argyrou, T. D. O'Rourke, H. E. Stewart, and B. P. Wham, "Large-scale fault rupture tests on pipelines reinforced with cured-in-place linings," *Journal of Geotechnical and Geoenvironmental Engineering*, vol. 145, no. 3, Article ID 04019004, 2019.

[20] C. Argyrou, D. Bouziou, T. D. O'Rourke, and H. E. Stewart, "Retrofitting pipelines with cured-in-place linings for earthquake-induced ground deformations," *Soil Dynamics and Earthquake Engineering*, vol. 115, pp. 156–168, 2018.

[21] J. Lee and G. L. Fenves, "Plastic-damage model for cyclic loading of concrete structures," *Journal of Engineering Mechanics*, vol. 124, no. 8, pp. 892–900, 1998.

[22] H. Fang, B. Li, F. Wang, Y. Wang, and C. Cui, "The mechanical behaviour of drainage pipeline under traffic load before and after polymer grouting trenchless repairing," *Tunnelling and Underground Space Technology*, vol. 74, pp. 185–194, 2018.

[23] General Administration of Quality Supervision, *Inspection and Quarantine of the People's Republic of China, Concrete and Reinforced Concrete Sewer Pipes (GB/T 11836-2009)*, Standards Press of China, Beijing, China, 2009.

[24] M. Oualit, R. Jauberthie, F. Rendell, Y. Melinge, and M. T. Abadlia, "External corrosion to concrete sewers: a case study," *Urban Water Journal*, vol. 9, no. 6, pp. 429–434, 2012.

[25] Ministry of Housing and Urban-Rural Development of the People's Republic of China, *Technical Specification for Trenchless Rehabilitation and Renewal of Urban Sewer Pipeline (CJJ/T210-2014)*, China Architecture & Building Press, Beijing, China, 2014.

[26] ASTM, *1216 Standard Practice for Rehabilitation of Existing Pipelines and Conduits by the Inversion and Curing of a Resin-Impregnated Tube*, American Society for Testing and Materials, West Conshohocken, PA, USA, 1993.

[27] Z. M. Wang, *Study on mechanical behaviors of buried pipelines under traffic loads*, Ph.D. thesis, Zhejiang University, Zhejiang, China, 2006.

[28] Ministry of Construction of the People's Republic of China, *Structural Design Code for Special Structures of Water Supply and Waste Water Engineering (GB 50332-2002)*, China Architecture & Building Press, Beijing, China, 2002.

[29] B. Li, H. Fang, H. He, K. Yang, C. Chen, and F. Wang, "Numerical simulation and full-scale test on dynamic response of corroded concrete pipelines under Multi-field coupling," *Construction and Building Materials*, vol. 200, pp. 368–386, 2019.

[30] Ministry of Housing and Urban-Rural Development of the People's Republic of China, *Code for Design of Outdoor Wastewater Engineering (GB 50014-2006)*, China Planning Press, Beijing, China, 2006.

[31] J. Wang and Z. Yang, "Axial friction response of full-scale pipes in soft clays," *Applied Ocean Research*, vol. 59, pp. 10–23, 2016.

[32] M. Xu, D. Shen, and B. Rakitin, "The longitudinal response of buried large-diameter reinforced concrete pipeline with gasketed bell-and-spigot joints subjected to traffic loading," *Tunnelling and Underground Space Technology*, vol. 64, pp. 117–132, 2017.

[33] G. F. An, "Optimal design of the cured-in-place pipe lining for trenchless rehabilitation of drainage pipelines," *Geological Science and Technology Information*, vol. 2, pp. 1–9, 2016.